Atomic scale study of TbCo2.5/Fe multilayers by laser-assisted tomographic atom probe

A. Grenier, R. Larde, E. Cadel, F. Vurpillot, J. Juraszek, J. Teillet, Nicolas Tiercelin

Atomic-scale study of $TbCo_{2.5}/Fe$ multilayers by laser-assisted tomographic atom probe

Cite as: J. Appl. Phys. **102**, 033912 (2007); https://doi.org/10.1063/1.2761825
Submitted: 18 August 2006 • Accepted: 13 June 2007 • Published Online: 06 August 2007

A. Grenier, R. Lardé, E. Cadel, et al.

Atomic-scale study of $TbCo_{2.5}$/Fe multilayers by laser-assisted tomographic atom probe

A. Grenier, R. Lardé, E. Cadel, F. Vurpillot, J. Juraszek,[a] and J. Teillet
Groupe de Physique des Matériaux, UMR 6634 CNRS—Université de Rouen, BP 12, 76801 Saint Etienne du Rouvray Cedex, France

N. Tiercelin
LEMAC—IEMN, DOAE UMR CNRS 8520, Cité Scientifique, BP 69, 59652 Villeneuve d'Ascq, France

(Received 18 August 2006; accepted 13 June 2007; published online 6 August 2007)

Sputtered ($TbCo_{2.5}$ 25 nm/Fe 20 nm) multilayers have been analyzed by laser-assisted tomographic atom probe. It allowed us to perform three-dimensional reconstructions of the layers and to determine their composition at the atomic scale. From the concentration profiles inside the multilayer, we show that the diffused interfaces are not symmetric and that a stronger Fe-Co mixing is present at the top of the crystalline iron layers as compared to the top of amorphous TbCo layers.
 [DOI: 10.1063/1.2761825]

I. INTRODUCTION

In recent years, nanometric multilayers were extensively studied because of their interest for fundamental bidimensional magnetism and its applications.[1,2] Among them, magnetostrictive multilayers are active materials having the property to be deformed when submitted to an external magnetic field, opening the way for applications as actuators in microelectromechanical systems (MEMS).[3] Giant magnetostriction effect at room temperature is obtained in rare earth-transition metal (RE-TM) alloys, such as $TbFe_2$ or $TbCo_2$.[4–9] However, large deformation of these bulk materials requires large saturation magnetic field, limiting the field of applications. Strong reduction of the saturation field can be obtained by exchange coupling of RE-TM amorphous alloy layers having giant magnetostriction and soft magnetic TM alloy layers having low anisotropy and high saturation magnetization. Hence, high values of the magnetostrictive susceptibility have been reported in such exchange-coupled magnetostrictive multilayers.[10–14]

Due to the interdiffusion between layers at the interface during the deposition process, these multilayers generally have compositionally modulated interfaces. So, for small layer thicknesses, the properties of these materials will strongly depend on the interfacial/bulk thicknesses ratio in layers and will then strongly depend on both the thickness of the layers and the interface roughness. For instance, this was evidenced for magnetic properties such as perpendicular magnetic anisotropy in Fe/Tb multilayers.[15–18]

Up to now, the structural and microstructural properties of these magnetostrictive multilayers have been extensively investigated by conventional techniques [x-ray diffraction, transmission electron microscopy, Mössbauer spectroscopy (including ^{57}Fe probe monolayers), etc.]. Nevertheless, as far as we know, no precise information about the atomic scale compositional modulation was obtained.

To evidence the atomic-scale compositional modulation in these multilayers, we used the ultrahigh spatial resolution of the tomographic atom probe (TAP).[19] This technique provides a powerful method by which the chemistry of the interfaces can be observed at the atomic level. The principle of the atom probe is based on ionization and evaporation of surface atoms by field effect. The sample is a sharp needle with end radius in the range 10–50 nm. This rounded form is needed to achieve very high electric evaporation field (10–60 V/nm) at the surface of the specimen, which is created by applying a positive voltage of several kilovolts to the tip. In a conventional tomographic atom probe, the pulsed evaporation of atoms is obtained by the application of high-voltage pulses superimposed to the standing voltage. During the measurement, the specimen is successively field-evaporated layer by layer and the ions are collected by a position-sensitive 2D detector, giving the spatial positions of the tip atoms. The chemical identification of the field-evaporated ions is carried out by a time-of-flight mass spectrometer.[19] The lateral spatial resolution at the specimen surface is better than 0.5 nm and the depth resolution is close to 0.1 nm. These high resolutions allow investigation of metallic layers of a few nanometers thickness in terms of both chemical nature and atomic-scale features such as layer roughness. Comparison with other high-resolution analytical microscopies can be found in Ref. 20.

However, multilayered materials are difficult to analyze by conventional tomographic atom because of frequent sample rupture during voltage pulsing. This problem can be avoided by replacing the voltage pulse with a femtosecond laser pulse with a limited temperature rising, avoiding surface diffusion effects.[21,22] It was proven that both the spatial resolution and the composition measurement are not degraded with this type of instrument.[22]

So, the aim of this work is to characterize the compositional modulation in ($TbCo_{2.5}$ 20 nm/Fe 25 nm) multilayers at the atomic scale with a laser-assisted tomographic atomic probe (LATAP). To obtain the tip from the multilayered sample, we used a method described by Larson *et al.*,[23] based on a deposition of multilayers on Si posts and then

[a]Electronic mail: jean.juraszek@univ-rouen.fr

needle shaping of the posts using a focused ion beam (FIB) device. It must be noted that the thicknesses of the layers do not allow an efficient magnetic coupling between the layers, but they were chosen in order to study unambiguously either the center of layers or the interfaces.

II. EXPERIMENT

A. Preparation of the sample

The multilayer was prepared by the rf-sputtering method, using modified and automated Leybold Z550 equipment in a clean-room environment. The substrate is a silicon wafer patterned using standard optical lithography followed by deep-trench reactive ion etching in order to create square posts (width 10 μm, length 100 μm). Prior to deposition, the substrate was cleaned for 10 min in a standard $H_2O_2 + H_2SO_4$ solution, and another 10 min in a 10% HF solution to remove the residual contamination and silicon oxide. It was then thoroughly rinsed using deionized water and dried within a few minutes. Then, the Fe (25 nm thick) and TbCo (20 nm thick) layers were deposited by sputtering a pure Fe target and a composite $TbCo_{2.5}$ target, respectively. The composition of this composite target was previously measured by energy-dispersive x-ray (EDX) measurement. X-ray diffraction performed on the multilayer has shown that the Fe layers are crystallized in the bcc phase, while the TbCo layers are in amorphous state. The base pressure in the ultrahigh vacuum chamber was below 10^{-6} mbar, and the typical deposition pressure of the argon gas was in the 10^{-3} mbar range, with a rf sputtering power of 500 W, resulting in a 1 kV autopolarization. The substrates laid on a water-cooled rotary turntable were therefore maintained at room temperature. During the deposition, the samples were oscillating under the targets at a constant speed, allowing better control of the deposition rate. Samples contain 6 periods, the top layer being a Fe layer. Finally, the multilayer was capped with 50 nm of Cr for protection.

After deposition, the sample was needle-shaped using a FIB device. For that, the posts were picked off the wafer and glued to the end of a thin rod with an electrically conducting epoxy glue. Then, a 30 keV gallium beam with current of 10–500 pA was used for milling the square-based posts with annular patterns of decreasing inner diameter. At the end of milling, the curvature radius was about 50 nm.

B. Laser-assisted tomographic atom probe conditions

The specimens cooled down to 80 K were analyzed in an ultrahigh vacuum chamber at a pressure of 10^{-9} -10^{-10} mbar. The femtosecond laser pulse system is an amplified ytterbium-doped laser (AMPLITUDE SYSTEM s-pulse) with a pulse length of 350 fs at a wavelength of 1030 nm. Analyses were performed using an energy density of $\simeq 5$ μJ/pulse focused onto a $\simeq 0.1$ mm^2 spot at the apex of the specimen, with a maximum repetition rate of 10 kHz. In these conditions, the density power is equivalent to more than 20% of the high-voltage electrical pulse. As a result, preferential evaporation of atoms between pulses is avoided, ensuring no bias in composition. Details on the 3D-reconstruction protocol can be found elsewhere.[24]

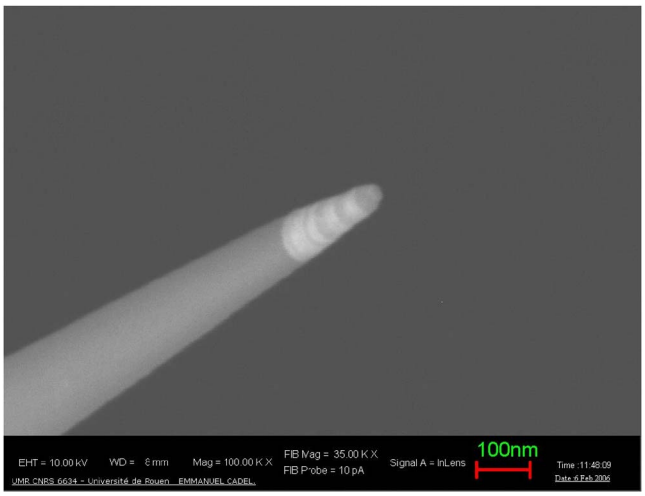

FIG. 1. SEM micrographs of a FIB needle-shaped sample of $TbCo_{2.5}$/Fe multilayer deposited on a Si post substrate.

III. RESULTS AND DISCUSSION

Figure 1 shows a scanning electron microscopy (SEM) micrograph of the sample after machining with the FIB. The picture gives evidence of a very nicely shaped tip with a periodic dark and white contrast on top. This contrast is due to the different electronic density between the layers (clear TbCo, dark Fe layers), indicating that the multilayer emerges from the tip apex. The number of observed bilayers corresponds to that of deposition, so the overall multilayer is still present on the post after machining. Nevertheless, the thickness of each layer is difficult to estimate from this picture, especially for the layers closest to the substrate.

The mass spectrum related to all the ions collected during the LATAP analysis of the multilayer is shown in Fig. 2(a). As expected, Fe, Co, and Tb ions are the main detected species in different charge states. In particular, the terbium is mainly observed in the form of oxides, hydrides, and hydroxides [Fig. 2(b)]. In addition, the observed hydrogen and oxygen peaks show a slight contamination of the sample from the residual gases (H_2, H_2O) from the vacuum preparation or analysis chambers. The analysis gives also evidence of the presence of Ga ions implanted during the needle-shaping process. However, a localized mass spectrum shows that the amount of Ga ions becomes negligible after a distance of about 20 nm from the top of the tip, so that only the first bilayer is damaged by Ga implantation. Finally, some argon ions (less than 0.4 at %), originating from the deposition by sputtering, are also detected in the whole analysis.

Figure 3 shows a 3D reconstruction of Tb, Co, and Fe ions in the middle part of the multilayer, i.e., far from the Ga ion implantation region. The reconstructed volume ($16 \times 16 \times 36$ nm^3) was oriented in order to image the interfaces perpendicular to the plane of view. Several Fe and TbCo layers are clearly seen, in agreement with the multilayered structure observed by SEM. The crystallinity of the Fe layers, evidenced by Mössbauer spectrometry and x-ray diffraction measurements,[25] cannot be revealed by the visualization of atomic planes. This can be the case in TAP analysis when there is a misorientation of the grain crystallographic orien-

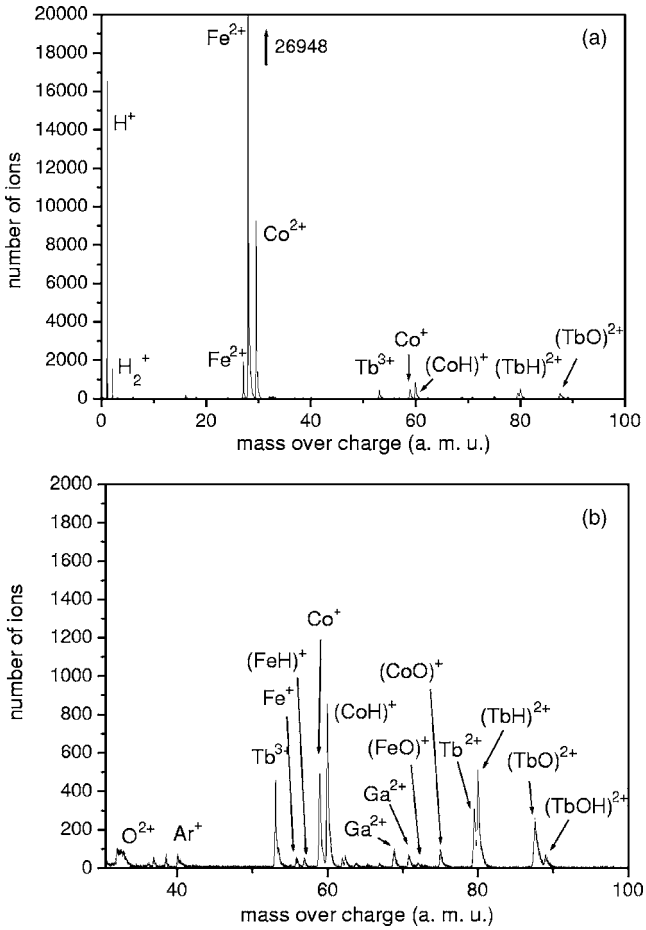

FIG. 2. Mass spectra related to the analysis of $TbCo_{2.5}$/Fe multilayers using the tomographicatom probe (a). Inset is the magnification in the 30–100 mass over charge range (b).

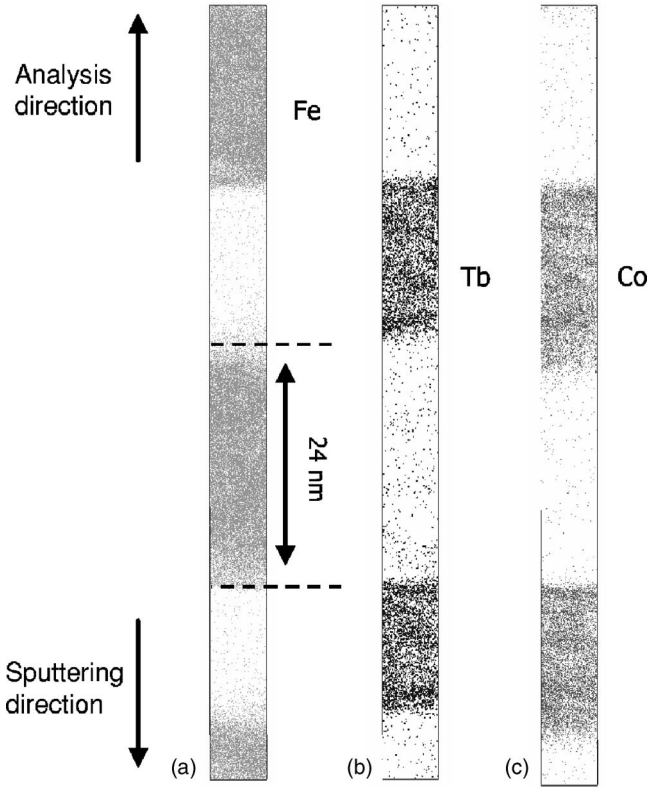

FIG. 3. Three-dimensional reconstruction of a given analyzed volume in a $TbCo_{2.5}$/Fe multilayer with different depicted atoms: (a) Fe; (b) Tb (including Tb oxides and hydrides); and (c) Co atoms. The volume was reoriented along the normal to interfaces.

tation with respect to the tip axis.[20] The reconstruction allows also visualization of the interfaces between the different layers. It is clearly seen that the interfaces at the top and the bottom of iron layers are different. The bottom interface is rather sharp, while the top one exhibits a stronger mixing between Fe and Co atoms.

The concentration profiles of the elements for a multilayer period are shown in Fig. 4. For sake of clarity, only oxygen, iron, cobalt, and terbium elements depth profiles are plotted, evidence for the modulation of composition of the multilayer. A high-purity (nearly 100 at %) is found for the core of Fe layers. For the core of TbCo layer, the measured Co and Tb concentrations are about 63% and 25%, respectively, giving a Co/Tb atomic ratio of about 2.5, in agreement with the measured composition of the sputtering TbCo target. This layer is also composed of oxygen ions (about 6 at % in the center of layers) and of some iron ions (about 3 at %). The distribution of Fe ions is quite homogeneous in all the TbCo layer, but oxygen ions are predominantly found at the interfaces. This effect is similar to oxygen segregation usually found at grain boundaries. The contamination of TbCo layers can be explained by the high reactivity of the rare earth (RE) with hydrogen and oxygen, which has been discussed in the case of thin films in a review.[26] A previous TAP study had already pointed out this contamination in sputtered Fe/Tb multilayers,[27] which was also observed by electron diffraction[28] or Auger electron spectroscopy.[29,30]

The different layer thicknesses have been measured at half concentration width of each element. The measured thicknesses of Fe, Tb, and Co layers are, respectively, 24.1±0.5, 19.0±0.5, and 19.9±0.5 nm, giving a multilayer period of 44.3±0.5 nm, in fair agreement with the nominal value (45 nm). This agreement points out the successful tip preparation process as compared to other methods such as

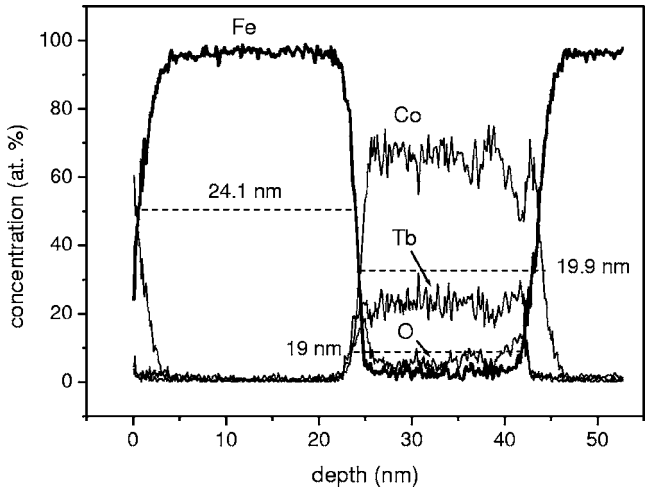

FIG. 4. Concentration depth profiles obtained perpendicular to the $TbCo_{2.5}$/Fe film planes.

depositing the multilayers directly onto a preformed tip substrate.[27] In the latter case, the control of the thickness of each individual layers is difficult, because the progressive decrease of the radius of curvature of the tip apex during deposition induces a reduction of the thickness of successive layers if the deposition rate is kept constant.

Different slopes of each element concentration profile can be found at the top and the bottom of Fe layers. In particular, the mixing between Co and Fe is stronger at the top as compared to the bottom of Fe layers, with average interfacial widths of 4 and 2 nm, respectively. On the other hand, the width of the mixed Tb-Fe region is only in the 1 nm range for both interfaces but appears slightly less at the top as compared to the bottom of Fe layers, in agreement with previous studies on Tb/Fe multilayers.[15,18] Such additional Co diffusion into the Fe layer was also observed by electron energy loss spectroscopy (EELS) in the case of annealed SmCo/Fe multilayers, where Co diffusion across interfaces was more significant in comparison with Sm diffusion.[31] In our case, mixing process occurring during deposition should be the main reason for the strong Fe-Co interdiffusion observed at only one interface. Thermal diffusion of Co in Fe is known to be low at room temperature because of small values of the coefficient diffusion, but enhanced diffusion has been reported in the case of thin films. Another effect could be mixing due to collisions of the incoming ions with the substrate atoms during deposition of the successive layers. The smaller and lighter Co and Fe atoms can travel, or be knocked in/out, longer distances than the larger and heavier Tb atoms. Sputtered Tb would contribute mostly to the momentum transfer and would be stopped faster. It is also probable that intermixing effect is more pronounced in the case of deposition on a crystalline material constituted of the lighter atoms (i.e., on a bcc Fe layer) than in the case of an amorphous material with high proportion of large heavy atoms (i.e., on a Tb-Co layer).

IV. CONCLUSION

This investigation has demonstrated the successful analysis of needle-shaped $TbCo_{2.5}$/Fe multilayers by LATAP. The values of the measured thickness and composition of the layers are in good agreement with the nominal ones. The atomic-scale reconstruction of the layers gives evidence of no symmetrical interfaces, with an enhanced diffusion of Co inside the top of the crystalline Fe layers as compared to the top of the amorphous TbCo layers. A study is in progress on multilayers with lower individual thicknesses for magnetostrictive applications.

ACKNOWLEDGMENTS

This work is supported by the European Community research program INTERREG IIIA No. 198. A. Grenier would thank the French Ministry of Research for a doctoral grant.

[1] *Ultrathin Magnetic Structures*, edited by B. Heinrich and J. A. C. Bland- (Springer, Berlin, 1994), Vols. I and II.
[2] *Metallic Multilayers*, edited by A. Chamberod and J. Hillairet (Trans Tech, Zurich, 1989).
[3] E. du Tremolet de Lacheisserie, J. Magn. Magn. Mater. **136**, 189 (1994).
[4] A. E. Clark and H. Benson, Phys. Rev. B **5**, 3642 (1972).
[5] Y. Nakamura, J. Magn. Magn. Mater. **31–34**, 829 (1983).
[6] N. H. Duc and D. Givord, J. Magn. Magn. Mater. **157–158**, 169 (1996).
[7] J. Betz, Ph.D. thesis, Université de Grenoble (1997).
[8] J. Betz, K. MacKay, and D. Givord, J. Magn. Magn. Mater. **207**, 180 (1999).
[9] N. H. Duc, *Handbook on the Physics and Chemistry of Rare Earths* (North Holland, Amsterdam, 2001), Vol. 32.
[10] D. Givord, A. D. Santos, Y. Souche, J. Voiron, and S. Wüchner, J. Magn. Magn. Mater. **121**, 216 (1993).
[11] S. Wüchner, J. Voiron, J. C. Toussaint, and J. J. Préjean, J. Magn. Magn. Mater. **148**, 264 (1995).
[12] D. Givord, J. Betz, K. MacKay, J. C. Toussaint, J. Voiron, and S. Wüchner, J. Magn. Magn. Mater. **159**, 71 (1996).
[13] E. Quandt, A. Ludwig, J. Betz, K. Mackay, and D. Givord, J. Appl. Phys. **81**, 5420 (1997).
[14] N. Tiercelin, J. B. Youssef, V. Preobrazhensky, P. Pernod, and H. LeGall, J. Magn. Magn. Mater. **249**, 519 (2002).
[15] J. Juraszek, A. Fnidiki, J. Teillet, F. Richomme, and M. Toulemonde, Solid Solid. State Commun. **106**, 83 (1998).
[16] J. Juraszek, A. Fnidiki, and J. Teillet, J. Appl. Phys. **84**, 379 (1998).
[17] F. Richomme, J. Teillet, A. Fnidiki, P. Auric, and P. Houdy, Phys. Rev. B **54**, 416 (1996).
[18] F. Richomme, B. Scholtz, R. A. Brand, W. Keune, and J. Teillet, J. Magn. Magn. Mater. **156**, 195 (1996).
[19] D. Blavette, B. Deconihout, A. Bostel, J. M. Sarrau, M. Bouet, and A. Menand, Rev. Sci. Instrum. **64**, 2911 (1993).
[20] D. Blavette, B. Deconihout, S. Chambreland, and A. Bostel, Ultramicroscopy **70**, 115 (1998).
[21] B. Gault, F. Vurpillot, A. Vella, M. Gilbert, A. Menand, D. Blavette, and B. Deconihout, Rev. Sci. Instrum. **77**, 043705 (2006).
[22] F. Vurpillot, B. Gault, A. Vella, M. Bouet, and B. Deconihout, Appl. Phys. Lett. **88**, 094105 (2006).
[23] D. J. Larson, A. K. Petford-Long, Y. Q. Ma, and A. Cerezo, Acta Mater. **52**, 2847 (2004).
[24] P. Bas, A. Bostel, B. Deconihout, and D. Blavette, Appl. Surf. Sci. **87–88**, 298 (1995).
[25] A. Grenier, R. Larde, E. Cadel, J. Le Breton, J. Juraszek, F. Vurpillot, N. Tiercelin, P. Pernod, and J. Teillet, J. Magn. Magn. Mater. **310**, 2215 (2007).
[26] M. Gasgnier, Phys. Status Solidi A **57**, 11 (1980).
[27] L. Veiller, F. Danoix, and J. Teillet, J. Appl. Phys. **87**, 1379 (2000).
[28] K. Cherifi, P. Donovan, C. Dufour, P. Mangin, and G. Marchal, Phys. Status Solidi A **122**, 311 (1990).
[29] G. Choe and R. M. Walser, Surf. Coat. Technol. **62**, 702 (1993).
[30] N. Sato, J. Appl. Phys. **59**, 2514 (1986).
[31] J. Zhang, Y. K. Takahashi, R. Gopalan, and K. Hono, Appl. Phys. Lett. **86**, 122509 (2005).